

NGP RESEARCH ON FIRE SUPPRESSION CHEMISTRY

Gregory T. Linteris
Fire Research Division, National Institute of Standards and Technology
Gaithersburg, MD 20899 USA
Tel: 301-975-2283; Fax: 301-975-4052; linteris@nist.gov

ABSTRACT

Several NGP projects studied the mechanisms of chemical suppressants, including those containing halogens, phosphorus, and metals. From the work, several general principles of chemical flame inhibition are outlined. The present paper describes the conditions for which a chemically active agent can be effective, and when it is most effective, and when it may not be effective. These general principles are demonstrated with numerical and experimental data and analyses for flame inhibition by various metals, halogens, phosphorus, and inert compounds, in premixed, counterflow diffusion, and cup-burner flames.

INTRODUCTION

The NGP research examining the effects of agent chemistry and flame inhibitor efficiency is outlined in references [1-13], and the present paper draws its material from those references. From that research, one can assemble some general principles of flame inhibition, and those basic principles are outlined here.

Two words commonly used to describe the influence of chemical additives on flames are inhibition and suppression. The term “suppression” refers to the extinguishment of a flame or fire, while the term “inhibition” describes a weakening of the flame, which may or may not lead to extinguishment. Whether a flame is only weakened or is completely extinguished through addition of an agent depends upon the amount of the agent applied, and how close the flame is to extinguishment to start with. That is, there is a balance between the time available for chemical reaction and the flow time, which are described by the extinction Damköhler number. Chemical additives typically work by increasing the chemical reaction time (i.e, lowering the overall reaction rate) so that the flame cannot be supported in the existing flow field [14]. While addition of any amount of chemical additive will weaken a flame, only a high enough concentration will extinguish it. As will be described below, the effectiveness of chemical additives is generally non-linear with agent concentration. Hence, the agent concentration of most interest is that which completely extinguishes the flame.

RESULTS AND DISCUSSION

Flame inhibitors generally work through two mechanisms: physical and chemical. Physical mechanisms involve dilution of the reactants, a change in the average specific heat of the reactant mixture per mass of fuel burned (which typically is the more important effect). Chemical effects change the overall reaction rate due to either trapping of the reactive chain-branching radicals (for example with fluorinated hydrocarbons), or catalytic cycles (for example with HBr) which effectively recombine the radicals into less reactive species. Agents that enter

into catalytic cycles are more interesting, since far lower concentrations of these species are required to suppress fires. One might reasonably ask the question: “When is a catalytic inhibitor effective?” Answering this question is the goal of the present paper.

Catalytic flame inhibitors are effective when they get to the right place in the flame, at the right time, in the right form, and can then lower the volume fraction of chain-carrying radicals (O, H, and OH). Since we are dealing here with steady flames, the time part is not relevant (but could be in other situations). Each of these requirements is discussed below.

AGENT LOCATION FOR EFFECTIVE INHIBITION

Overview

The most effective location for a flame inhibitor is where the radicals are. This is where the catalytic agents recombine the radicals, and consequently is where the active species need to be delivered. From both experimental measurements (see Figure 1, Figure 2, and Figure 3) and calculations (see Figure 4, bottom frame), it is known that catalytic agents reduce radical concentrations. Also, catalytic agents are most effective when their active species overlap in space with the peak radical volume fractions (see Figure 5).

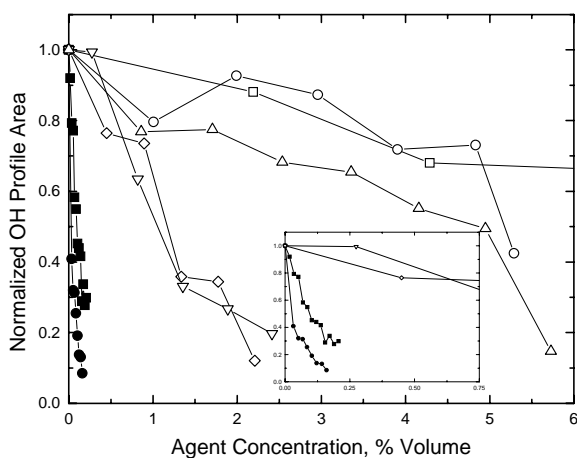


Figure 1. Normalized OH LIF profile areas versus inhibitor agent delivery concentrations propane-air counterflow diffusion flame. Data legend: (□) N₂, (O)FM-200, (Δ)FE-36, (▽)PN, (◇)CF₃Br, (■)DMMP, and (●)Fe(CO)₅. Insert: plot of the PN, CF₃Br, DMMP, and Fe(CO)₅, data for agent concentration up to 0.75 % volume. From ref. [10].

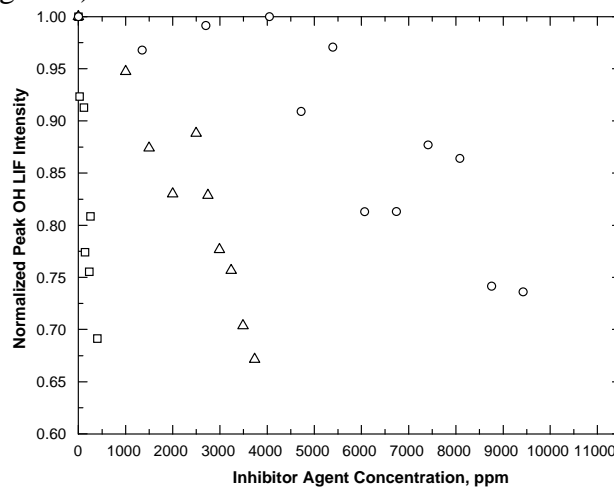


Figure 2. Dependence of normalized maximum OH LIF intensity on inhibitor concentration in a low-pressure CH₄-air counterflow diffusion flame. Symbols: (□)Fe(CO)₅, (Δ)CF₃Br, (O)N₂. From ref. [11].

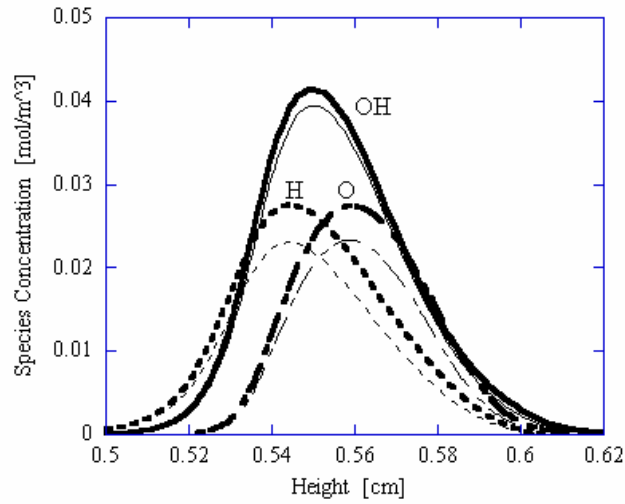


Figure 3. Effect of 572 ppm of DMMP on calculated OH, H, and O concentration profiles in Flame 1 ($\text{CH}_4/\text{O}_2/\text{N}_2$). Dark lines are undoped profiles and thin lines are with DMMP addition. From ref. [8].

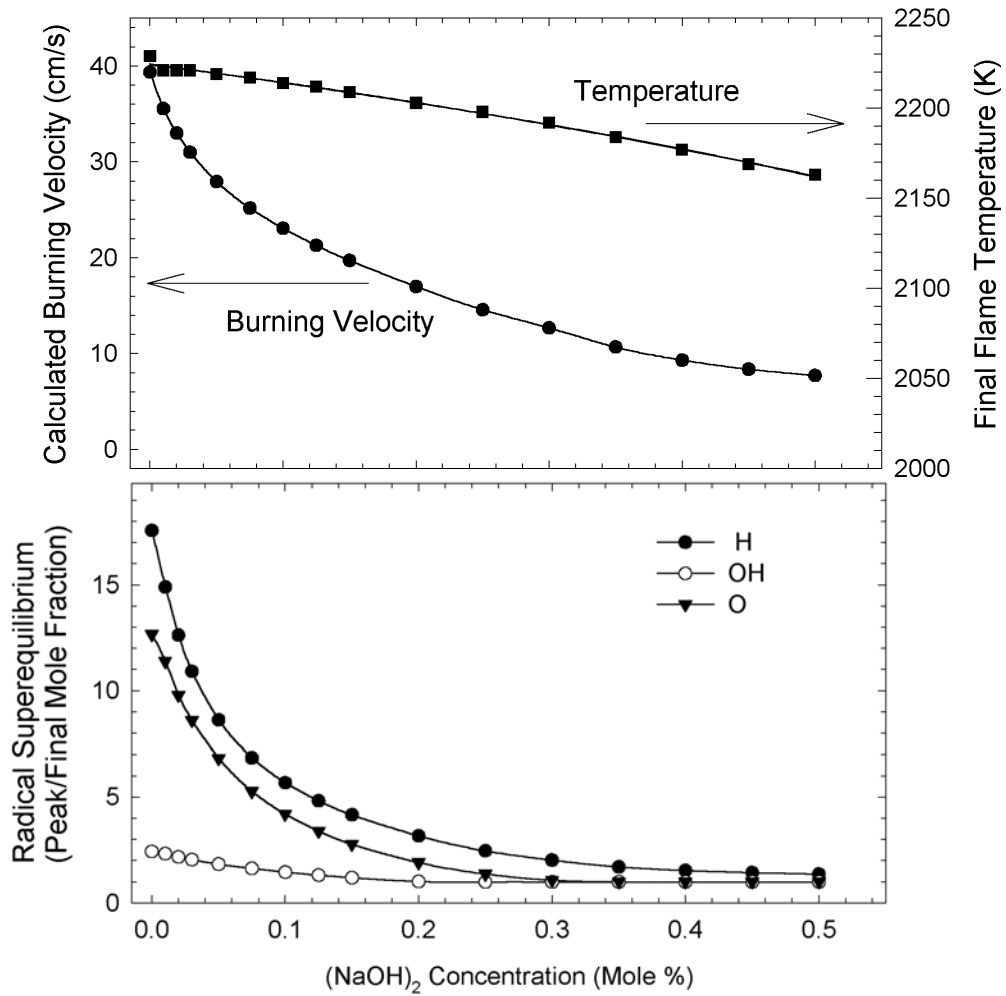


Figure 4. Burning velocity, temperature, and super-equilibrium ratio of flame radicals computed for atmospheric pressure stoichiometric methane/air mixtures inhibited by sodium hydroxide. From ref. [12].

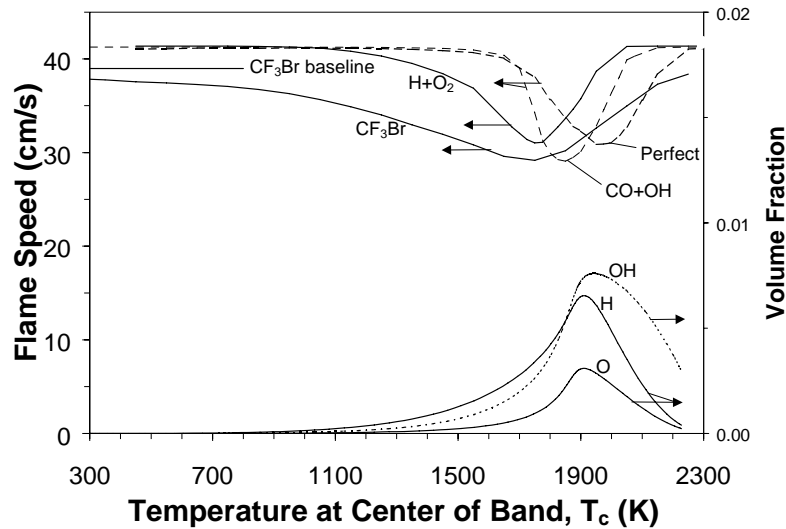


Figure 5. Variation of flame speed (left axis) for four types of perturbation: reduction of the $\text{H}+\text{O}_2 \leftrightarrow \text{OH}+\text{O}$ or $\text{CO}+\text{OH} \leftrightarrow \text{CO}_2+\text{H}$ reaction rate, and inhibition by a perfect agent or CF_3Br . The “ CF_3Br baseline” refers to the flame speed when the halogen chemistry is damped by 10^{-4} . The band width Δ is 300 K, so the band extends 150 K below and above the temperature shown on the x-axis. The calculated volume fraction of OH, H, and O (right axis) is shown for an uninhibited stoichiometric methane-air flame. From ref. [13].

Superequilibrium

The effectiveness of a given agent at the location of peak radical volume fraction is dependent upon the degree of radical super-equilibrium. Catalytic agents speed up the movement of a chemical system that is out of equilibrium to equilibrium but do not modify the equilibrium conditions themselves. As Figure 4 (bottom frame) shows, the uninhibited premixed methane-air flame has superequilibrium ratios of 2.5 to 18, and the degree of inhibition (marginal change in slope of the burning velocity in top frame) is decreased as the super-equilibrium ratio decreases. Also, as shown in Figure 6 (for premixed CH_4 -air flames at various fuel-air ratios and oxygen volume fraction, which change the super-equilibrium ratio), as the degree of radical super-equilibrium increases, the inhibition effect for a given amount of agent is also larger. For counterflow diffusion flames, the amount of strain (i.e., gas velocities) affects the degree of radical super-equilibrium is shown in Figure 7.

A consequence of the need for radical super-equilibrium is that the effectiveness of catalytic agents varies with the temperature of the flame. This is illustrated indirectly in Figure 6 (since the super-equilibrium is highest in the lowest temperature flames), and directly in Figure 8, which shows the measured effectiveness (from extinction strain rate or $[\text{OH}]$ reduction) in counterflow diffusion flames as a function of flame temperature. Nonetheless, to reach the location of peak radical volume fraction in a system with radical super-equilibrium, effective agent transport is required.

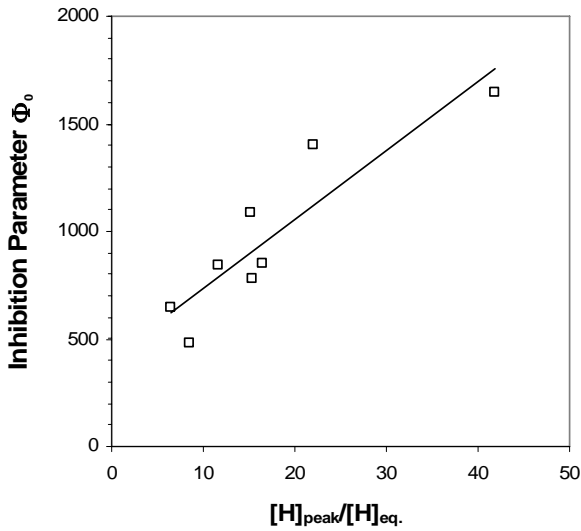


Figure 6. Variation of inhibition parameter Φ_0 [15] with degree of H-atom super equilibrium in premixed methane-air flames with added $\text{Fe}(\text{CO})_5$. Data from ref. [16].

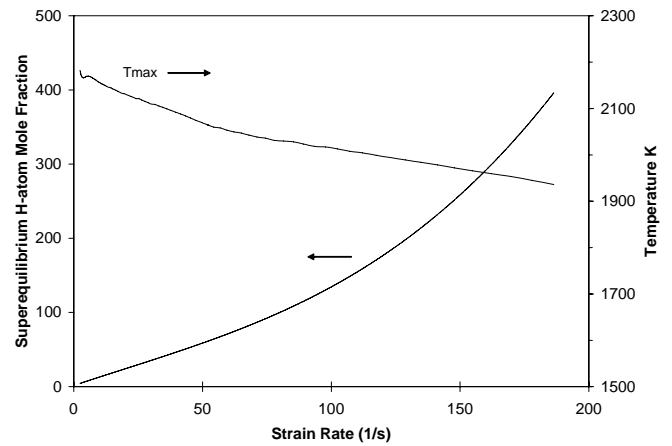


Figure 7. Degree of H-atom super-equilibrium and peak temperature as a function of strain rate for a CH_4 -air counterflow diffusion flame.

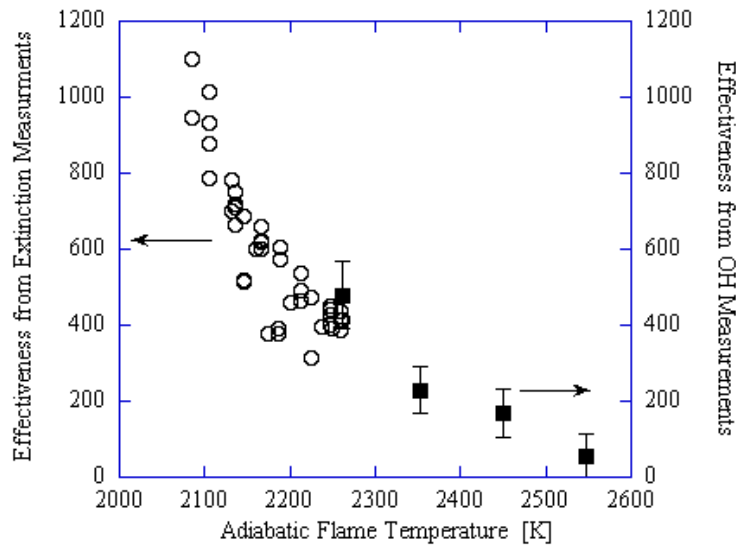


Figure 8. Temperature dependence of phosphorus agent effectiveness. Open circles are effectiveness data defined in terms of reduction of global extinction strain; filled squares are effectiveness data in terms of reduction in OH concentration) From ref. [8].

AGENT TRANSPORT

In order for a chemical agent to reach the region of peak radical volume fraction, it must be transported there. The efficiency of this process depends on the phase of the agent (solid, liquid or gas), and the location of agent addition relative to the flame and peak radical volume fractions.

The agent transport occurs primarily through convection or diffusion, and can be helped or hindered by thermophoresis (or thermal diffusion for gases). Figure 9 shows a counterflow diffusion flame with the flame (indicated by the blue line) on either the fuel or oxidizer side of the stagnation plane (indicated by the horizontal dotted line). This is achieved in practice by diluting the fuel and air stream (and is described by the varying stoichiometric mixture fraction). If agent is added to the side of the stagnation plane where the flame is, the agent convects through the flame; otherwise, it can only reach the flame by gaseous diffusion. If the agent is in the form of

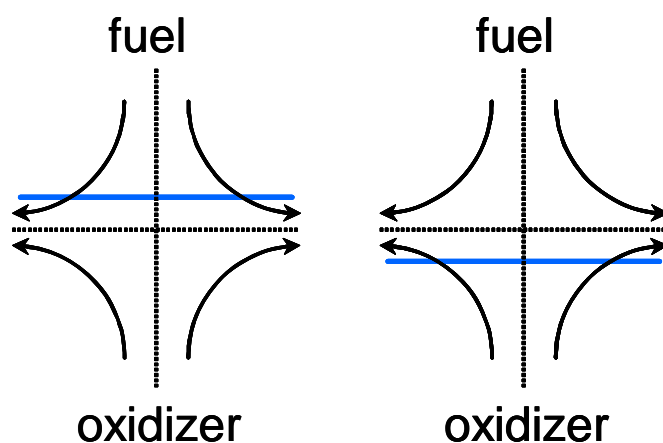


Figure 9. Counterflow diffusion flame with flame on fuel or oxidizer side of stagnation plane.

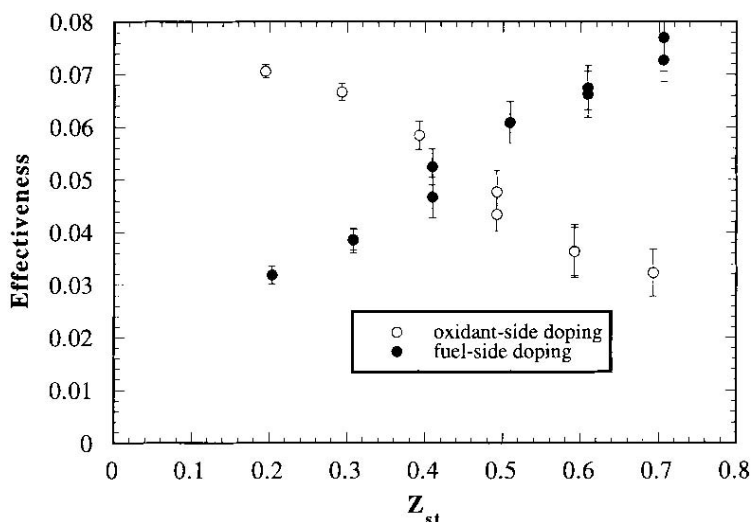


Figure 10. Flame suppression effectiveness of 25,000 ppm argon as an oxidant-side or fuel-side additive vs. stoichiometric mixture fraction. Effectiveness is defined as $((a_{q0} - a_q)/a_{q0})$. Flames are methane/nitrogen vs. oxygen/nitrogen; $a_{q0} = 350 \pm 10 \text{ s}^{-1}$. From ref. [7]

particles, they cannot diffuse, are entrained by the flow, and are susceptible to thermophoresis and momentum effects if they are large. The dependence of agent efficiency on the stoichiometric mixture fraction (i.e., flame location) is illustrated for a thermally acting agent (Ar) in Figure 10.

ACTIVE MOITIES FOR FLAME INHIBITION

Formation

To be effective, the agent must also be present as the correct chemical compounds (which usually are not the form in which the agent is added). This means that the agent must break down in the flame, form species which are active in the catalytic cycle, and then not be lost to other non-active forms. For iron, the for inhibition has been shown to occur in the gas phase, and is believed to procede as indicated in Figure 11. First, the inhibitor molecule itself (in this case $\text{Fe}(\text{CO})_5$) must break down. Often, the rate of decomposition of the initial inhibitor molecule is not limiting, over a wide range of activation energy (see Figure 12). Second, in addition to being transported to the location of peak radicals, the breakdown products must be able to react with other species to form those active in the inhibition cycle. For iron, in the usually more important H-atom cycle, the species FeO , FeOH , and $\text{Fe}(\text{OH})_2$ must be present in the gas phase in the region of the flame with highest radical volume fraction. Thus, Fe must be able to react with O_2 to form FeO_2 , which must then have access to O to form FeO . In some cases [17] this can be a limitation. Third, for inhibitors added as particles, they must have sufficient residence time to evaporate in the high-temperature region of the flame to deliver the active species [18].

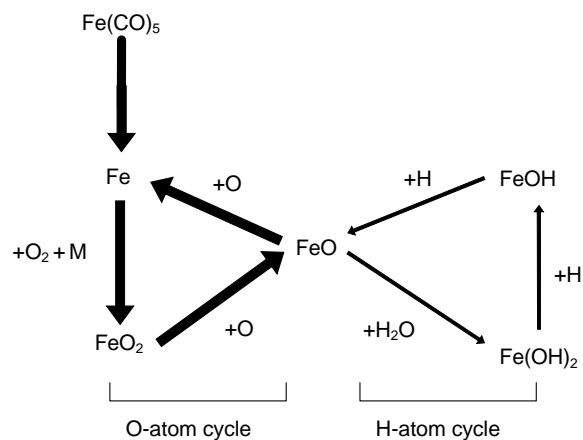


Figure 11. Schematic of iron inhibition cycle.

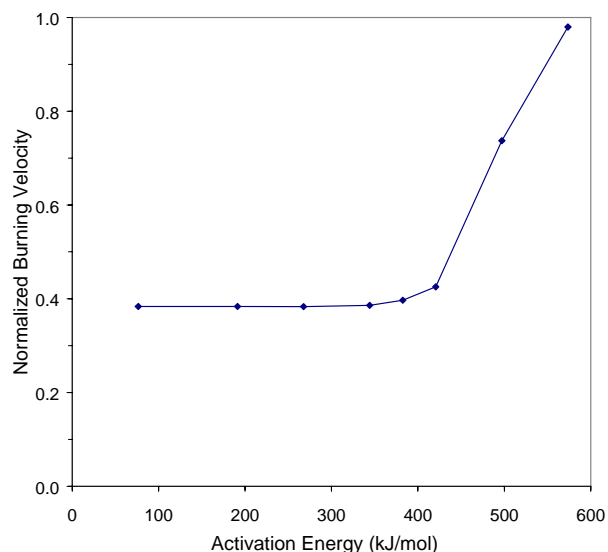


Figure 12. The normalized burning velocity of stoichiometric $\text{CH}_4/\text{O}_2/\text{N}_2$ flames at 400 ppm of ferrocene as a function of the activation energy of the one-step ferrocene decomposition reaction. From ref. [19].

Properties of Active Species

For the most effective chemical flame inhibition, the reaction rates within the catalytic cycle must be very fast (approaching gas-kinetic rates, with near zero activation energy, and near thermally neutral). This has also been discussed in the context of the bond energies of the inhibiting species [20]. It also helps if there are multiple catalytic cycles for a given element [21]. Finally, the cycle must be complete, in that the inhibiting species are regenerated [22].

Loss Mechanisms

To remain effective, the active species must not be subject to loss mechanisms. These can include condensation to particles [23, 24], loss to inactive gas-phase species [19], or shifting of the equilibrium constant for the active species [25-27]. The loss of effectiveness at higher concentrations and concurrent formation of particles for $\text{Fe}(\text{CO})_5$ added to premixed flames is shown in Figure 13, and in counterflow diffusion flames in Figure 14. The loss of effectiveness of NaOH in water droplets (possible due to condensation of NaOH) is shown in Figure 15. The loss of iron compounds to Fe_xF_y compounds in flames with added $\text{Fe}(\text{CO})_5$ and CF_3H is shown in Figure 16. Finally, the shifting in the equilibrium products for an Mn-inhibited flame is shown in Figure 17, in which the volume fraction of $\text{Mn}(\text{OH})_2$, a necessary intermediate species in the catalytic cycle, is shown to decrease in volume fraction at higher temperature, which leads to lower effectiveness, (but greater effectiveness at lower temperature as compared to iron).

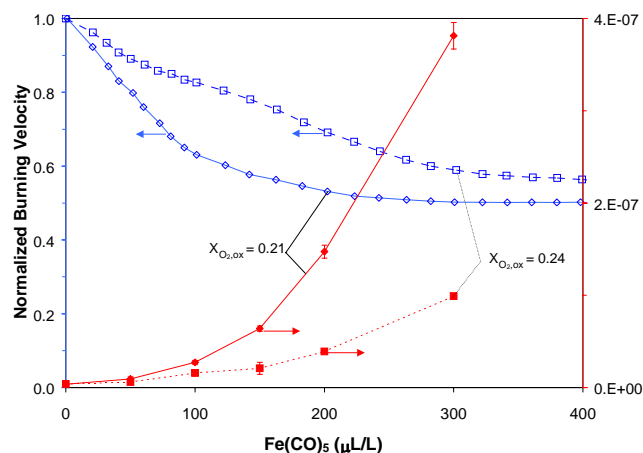


Figure 13. Normalized burning velocity (from Ref. [16]) and maximum Q_{vv} for $\phi=1.0$ CH_4 flame with $X_{\text{O}_2, \text{ox}} = 0.21$ and 0.24 (from ref.: [23]).

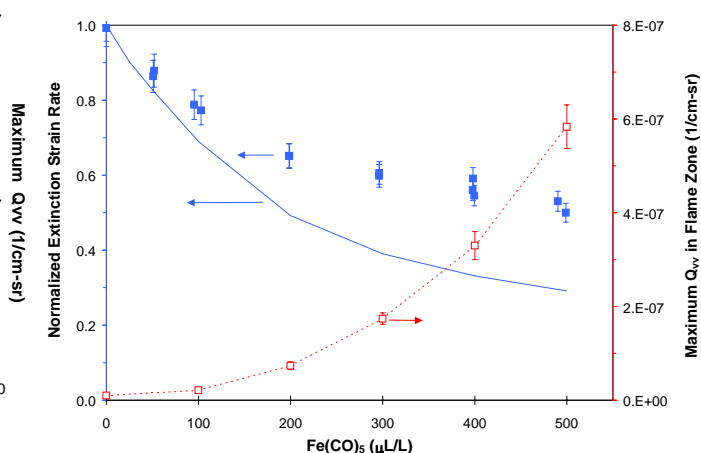


Figure 14. Correlation between inhibition effect and maximum scattering signal Q_{vv} . Filled points are experimental normalized a_{ext} , solid line is calculated a_{ext} ([17]). Open symbols connected by dotted lines are maximum measured Q_{vv} . Particle data collected at 75 % of a_{ext} (from ref.: [24]).

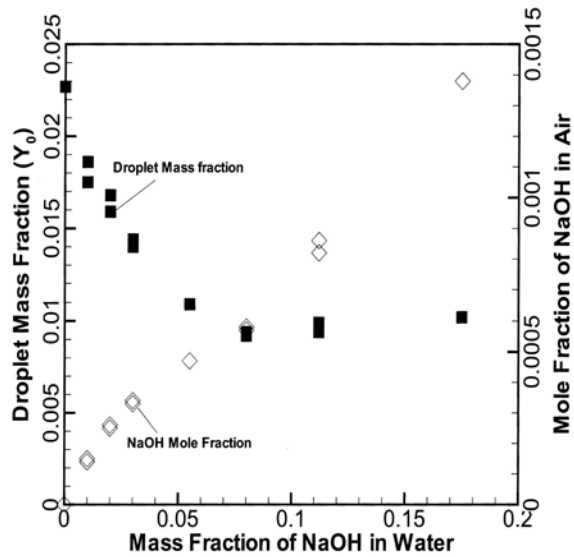


Figure 15. Y_0 and mole fraction of NaOH in air as a function of y_{NaOH} , for the extinction strain of 125 s^{-1} . From ref. [28].

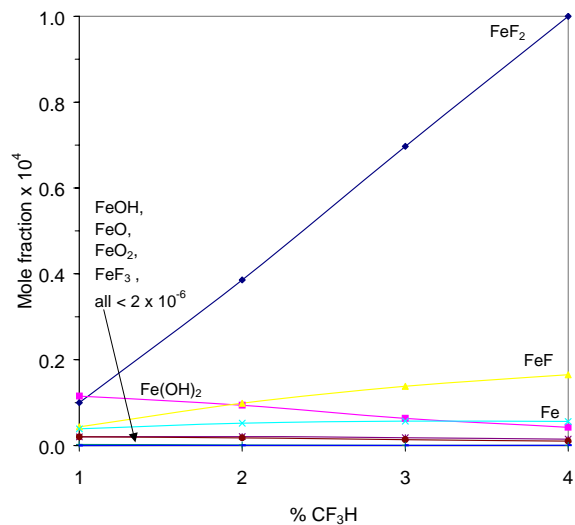


Figure 16 – Equilibrium mole fraction of active inhibiting species (Fe, FeO, FeOH, $\text{Fe}(\text{OH})_2$) and iron-fluorine species with 1 % to 4 % CF_3H (containing 0.35 % ferrocene) added to a stoichiometric methane-air reaction mixture. From ref. [19].

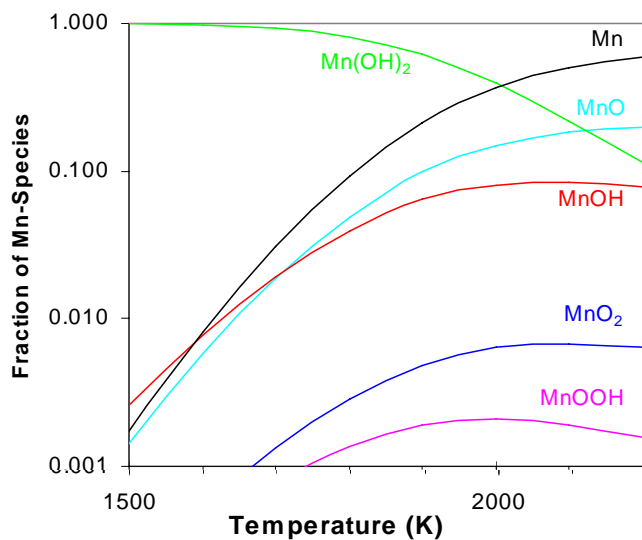


Figure 17. Fraction of Mn-species at equilibrium as a function of temperature in methane-air flames. From ref. [27].

THE PERFECT FLAME INHIBITOR

A model was developed of a perfect flame inhibitor [22]. In it, the inhibitor is added in its effective form, is a gas, is non-condensing, and reacts only with the chain-branching flame radicals (i.e., it is non-reacting with all other species). The perfect inhibitor model is written in terms of the following two reactions: $X + In = InX$, and $X + InX = X_2 + In$, where X is the major chain carrier and In is the inhibiting species. Both scavenging and regeneration reactions are termination processes. Thus the perfect catalytic recombination cycle is the most effective one due to termination of chain carriers at each reaction step of the catalytic cycle, and due to gas-kinetic rates for these reactions. Similarly, a perfect heterogeneous model was developed for flame inhibition by particles [23]. In it, all collisions of radicals with the particles effectively recombine the radicals into stable species. Figure 18 shows the predicted burning velocity reduction caused by a perfect gas-phase inhibitor, or a perfect heterogeneous inhibitor, together with experimental data for $Fe(CO)_5$. As shown, the perfect inhibitor model will always have a higher efficiency than the perfect heterogeneous model. Interestingly, the efficiency of $Fe(CO)_5$ is relatively close to that of the perfect gas-phase inhibitor. As indicated in Figure 5, the perfect inhibitor model shows that for premixed flames, the region where inhibition is most effective is where the radicals are located. For CF_3Br , the region of maximum effectiveness is also close to the region of peak radical volume fraction, but it's effectiveness there is limited by the equilibrium relationship for the reaction $HBr + H = H_2 + Br$, which shifts to the right at higher temperature, so that HBr is no longer available for the key inhibition step.

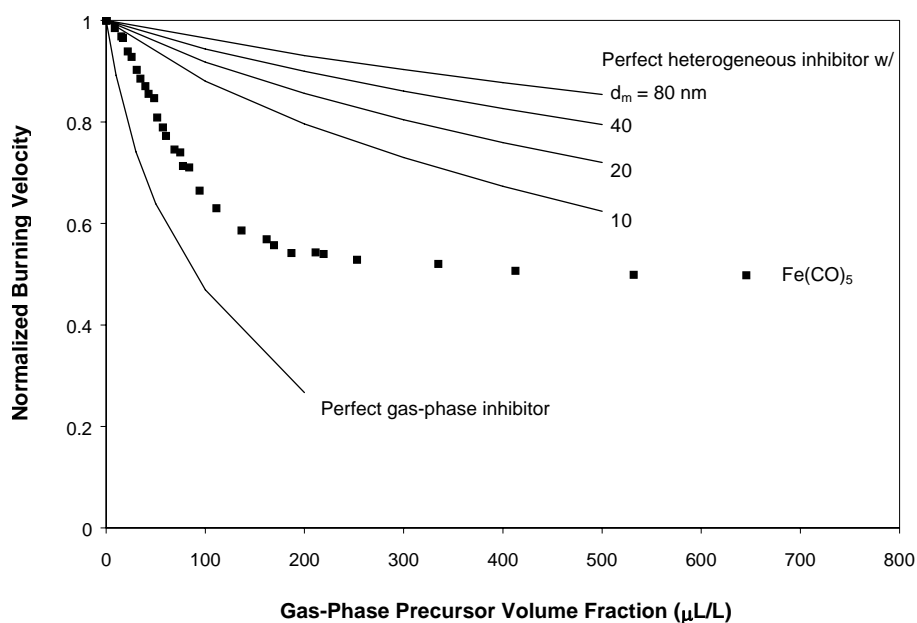


Figure 18. Calculated normalized burning velocity for several diameters d_m of ideal heterogeneous inhibitor. Also shown are $Fe(CO)_5$ data, and calculated normalized burning velocity using the perfect gas-phase inhibitor mechanism. From ref. [23]

CONCLUSIONS

Several properties which make chemical flame inhibitors effective or ineffective fire suppressants have been outlined. These have to do with both the properties of the flame, as well as of the inhibitor. Chemical suppressants have the potential to be up to two orders of magnitude more effective than CF_3Br . The difficult challenge is to devise methods to effectively deliver the active moieties to the radical production region of flames, and then keep them from condensing to particles, which are not as effective flame inhibitors.

ACKNOWLEDGMENT

This research was supported by the Department of Defense's Next Generation Fire Suppression Technology Program, funded by the DoD Strategic Environmental Research and Development Program, and by the Office of Biological and Physical Research, National Aeronautics and Space Administration, Washington, DC.

REFERENCES

1. Zegers, E. J. P., Williams, B. A., Fisher, E. M., Fleming, J. W., and Sheinson, R. S., "Suppression of Nonpremixed Flames by Fluorinated Ethanes Andpropanes," *Combust. Flame*, **121**, 471, 2000.
2. Linteris, G. T., "Limits to the Effectiveness of Metal-Containing Fire Suppressants", NISTIR 7177, 2004.
3. Linteris, G. T. and Chelliah, H. K., "Powder-Matrix Systems for Safer Handling and Storage of Suppression Agents", National Institute of Standards and Technology, NISTIR 6766, 2001.
4. Linteris, G. T., Rumminger, M. D., Babushok, V., Chelliah, H., Lazzarini, A. K., and Wanigarathne, P., "Effective Non-Toxic Metallic Fire Suppressants", National Institute of Standards and Technology, NISTIR 6875, 2002.
5. Tan, N. C. B. DeSchepper D. C. and Balogh, L., "Dendritic Polymers as Fire Suppressants ", ARL-TR-2071, 1999.
6. Macdonald, M. A., Jayaweera, T. M., Fisher, E. M., and Gouldin, F. C., "Inhibition of Nonpremixed Flames by Phosphorus-Containing Compounds," *Combust. Flame*, **116**, 166, 1999.
7. MacDonald, M. A., Jayaweera, T. M., Fisher, E. M., and Gouldin, F. C., "Variation of Chemically Active and Inert Flame-Suppression Effectiveness with Stoichiometric Mixture Fraction," *Proceedings of the Combustion Institute*, Vol. 27, The Combustion Institute, p. 2749, 1998.
8. Macdonald, M. A., Gouldin, F. C., and Fisher, E. M., "Temperature Dependence of Phosphorus-Based Flame Inhibition," *Combust. Flame*, **124**, 668, 2001.
9. Nogueira, M. F. M. and Fisher, E. M., "Effects of Dimethyl Methylphosphonate on Premixed Methane Flames," *Combust. Flame*, **132**, 352, 2003.
10. Skaggs, R. R., Daniel, R. G, Miziolek, A. W., McNesby, K. L., Babushok, V. I., Tsang, W., and Smooke, M. D., "Spectroscopic Studies of Inhibited Opposed-Flow Propane-Air Flames," *Halon Options Technical Working Conference*, 117, 1999.
11. Skaggs, R. R., McNesby, K. L., Daniel, R. G., Homan, B., and Miziolek, A. W., "Spectroscopic Studies of Low Pressure Opposed Flow Methane/Airflames Inhibited by $\text{Fe}(\text{Co})(5)$, Cf_3br , or N-2," *Combust. Sci. Technol.*, **162**, 1, 2001.
12. Williams, B. A. and Fleming, J. W., "CF₃Br and Other Suppressants: Differences in Effects on Flame Structure," *Proc. Combust. Inst.*, **29**, 345, 2003.
13. Rumminger, M. D., Babushok, V. I., and Linteris, G. T., "Temperature Regions of Optimal Chemical Inhibition of Premixed Flames," *Proc. Combust. Inst.*, **29**, 329–336, 2002.
14. Williams, F. A., "A Unified View of Fire Suppression," *J. Fire Flammability*, **5**, 54, 1974.

15. Fristrom, R. M. and Sawyer, R. F., "Flame Inhibition Chemistry," *AGARD Conference Proceedings No. 84 on Aircraft Fuels, Lubricants, and Fire Safety, AGARD-CP 84-71*, North Atlantic Treaty Organization, p. 12 to 12-17, 1971.
16. Reinelt, D. and Linteris, G. T., "Experimental study of the inhibition of premixed and diffusion flames by iron pentacarbonyl," *Proc. Combust. Inst.*, **26**, 1421, 1996.
17. Rumminger, M. D. and Linteris, G. T., "Numerical Modeling of Counterflow Diffusion Flames Inhibited by Iron Pentacarbonyl," *Fire Safety Science: Proc. of the Sixth Int. Symp.*, Int. Assoc. for Fire Safety Science, p. 289, 2000.
18. Chelliah, H. K., "Flame Inhibition/Suppression by Water Mist: Droplet Size/Surface Area, Flame Structure, and Flow Residence Time Effects.," *Proc. Combust. Inst.*, **31**, in press, 2006.
19. Linteris, G. T., Rumminger, M. D., Babushok, V., and Tsang, W., "Flame Inhibition by Ferrocene and Blends of Inert and Catalytic Agents," *Proc. Combust. Inst.*, **28**, 2965, 2000.
20. Williams, B. A. and Fleming, J. W., "Influence of Bond Energies on Catalytic Flame Inhibition: Implications for the Search for New Fire Suppressants", NRL/MR/618003-8728, 2003.
21. Kellogg, C. B. and Irikura, K. K., "Gas-Phase Thermochemistry of Iron Oxides and Hydroxides:Portrait of a Super-Efficient Flame Suppressant," *Journal of Physical Chemistry a*, **103**, 1150, 1999.
22. Babushok, V. , Tsang, W., Linteris, G. T., and Reinelt, D., "Chemical limits to flame inhibition," *Combust. Flame*, **115**, 551, 1998.
23. Rumminger, M. D. and Linteris, G. T., "The Role of Particles in the Inhibition of Premixed Flames by Iron Pentacarbonyl," *Combust. Flame*, **123**, 82, 2000.
24. Rumminger, M. D. and Linteris, G. T., "The Role of Particles in the Inhibition of Counterflow Diffusion Flames by Iron Pentacarbonyl," *Combust. Flame*, **128**, 145, 2002.
25. Day, M. J., Stamp, D. V., Thompson, K., and Dixon-Lewis, G., "Inhibition of Hydrogen-Air and Hydrogen-Nitrous Oxide Flames by Halogen Compounds," *Proc. Combust. Inst.*, **13**, 705, 1971.
26. Dixon-Lewis, G. and Simpson, R. J., "Aspects of Flame Inhibition by Halogen Compounds," *Proc. Combust. Inst.*, **16**, 1111, 1977.
27. Linteris, G. T., Knyazev, K., and Babushok, V., "Inhibition of Premixed Methane Flames by Manganese and Tin Compounds," *Combust. Flame*, **129**, 221, 2002.
28. Chelliah, H. K., Lazzarini, A. K., Wanigarathne, P. C., and Linteris, G. T., "Inhibition of Premixed and Non-Premixed Flames with Fine Droplets of Water and Solutions ," *Proc. Combust. Inst.*, **29**, 369, 2002.